nutraceuticals

MDPI

Article

Comparative Study of Anti-Inflammatory and Antimicrobial Potentials of Natural By-Products

Na-Hyeon Park [1,†], Ji-A Byeon [2,†], Moon-Pil Jung [1], Ju-Young Kim [1], Seulki Yoon [3], Gyu Hoon Kim [4], Bo-Ae Kim [5] and Yong-Jin Kwon [1,2,*]

[1] Department of Cosmetic Science, Kyungsung University, Busan 48434, Republic of Korea; anna461004@ks.ac.kr (N.-H.P.)
[2] Department of Cosmeceutical Science, Kyungsung University, Busan 48434, Republic of Korea; bzia@ks.ac.kr
[3] OATC Skin Clinical Trial Center, Seoul 08511, Republic of Korea
[4] Skinhealth Cosmetic Co., Ltd., Busan 48055, Republic of Korea
[5] Department of Cosmetics, College of Health and Safety Science, Mokwon University, Daejeon 35349, Republic of Korea
* Correspondence: yongjin@ks.ac.kr; Tel.: +82-51-663-5682
† These authors contributed equally to this study.

Abstract

Natural by-products (NBPs), including pomace, peels, stems, and skins, account for over 50% of materials generated during fresh fruit processing. Most of these are discarded or landfilled, contributing to environmental pollution. NBPs are rich in bioactive compounds, including polyphenols and flavonoids, suggesting their potential as functional ingredients for health promotion. Accordingly, twelve types of NBPs from Korea were extracted with 70% ethanol. Each extract was comparatively evaluated at a uniform concentration for antioxidant, tyrosinase inhibition, and elastase inhibition activities. Anti-inflammatory and antimicrobial activities were additionally evaluated to identify extracts with superior overall activity profiles. Based on these findings, four extracts exhibiting the highest activities were combined, and the NBP complex was further tested for its antioxidant, anti-inflammatory, and antimicrobial effects. Although certain individual NBPs extracts showed strong activities, the NBP complex exhibited enhanced overall effects. These findings indicate that selected NBPs, both individually and in combination, possess significant potential as health-promoting functional ingredients. The study provides scientific evidence supporting the valorization of fruit processing residues into value-added products while addressing environmental concerns associated with their disposal.

Keywords: natural by-products; anti-inflammatory; antimicrobial; functional compounds

Check for updates

Academic Editor: Ronan Lordan

Received: 29 November 2025
Revised: 13 February 2026
Accepted: 25 March 2026
Published: 30 March 2026

Copyright: © 2026 by the authors. Licensee MDPI, Basel, Switzerland. This article is an open access article distributed under the terms and conditions of the Creative Commons Attribution (CC BY) license.

1. Introduction

Natural by-products (NBPs), including pomace, peels, stems, and skins, account for more than 50% of the total biomass generated during fresh fruit processing. Most of these NBPs are disposed of through landfilling or incineration. However, these practices contribute to greenhouse gas emissions, including CO_2 and CH_4, and can result in the release of dioxins into the environment [1]. Meanwhile, NBPs are increasingly recognized as rich sources of valuable bioactive constituents, including polyphenols, flavonoids, and other phenolic compounds. Numerous studies have shown that extracts exhibit notable free-radical-scavenging capacity and antimicrobial activity against foodborne pathogens. Such evidence underscores the potential of these by-products to serve as functional ingredients

with diverse health-promoting effects [2,3]. Given these characteristics, these residual materials are enriched in bioactive constituents compared to the edible portions of fruits, suggesting their strong potential for value-added applications [4].

Based on these findings, the antioxidant and anti-inflammatory mechanisms of NBP-derived phytochemicals have been actively investigated. Inflammatory responses arise when tissues encounter harmful physical or chemical stimuli, leading to the upregulation of key mediators such as inducible nitric oxide synthase (iNOS) and cyclooxygenase-2 (COX-2), both of which play central roles in propagating inflammatory signaling [5]. Oxidative stress further increases iNOS expression, resulting in elevated nitric oxide (NO) production that readily reacts with reactive oxygen species (ROS) to generate peroxynitrite ($ONOO^-$), a highly reactive oxidant that exacerbates inflammatory tissue damage. In parallel, oxidative stress also upregulates COX-2, thereby promoting the production of downstream inflammatory mediators, including prostaglandins. Collectively, these oxidative stress–driven iNOS and COX-2 pathways form a mutually reinforcing cycle that intensifies oxidative damage and inflammatory responses [6,7].

Inflammatory responses can be triggered by pathogenic microorganisms that disrupt tissue homeostasis. Key pathogens, including *Staphylococcus aureus* (*S. aureus*), *Cutibacterium acnes* (*C. acnes*), and *Pseudomonas aeruginosa* (*P. aeruginosa*), activate pattern-recognition receptors and stimulate inflammatory signaling. Specifically, *C. acnes* promotes inflammation in the pilosebaceous unit [8,9], while *S. aureus* exacerbates atopic dermatitis through toxin-mediated immune activation [10,11]. *P. aeruginosa* sustains chronic inflammation via biofilm formation that impedes immune clearance [12,13]. Furthermore, opportunistic pathogens such as *E. coli*, *G. vaginalis*, and *C. albicans* contribute to secondary infections, cutaneous abscesses, or impaired barrier integrity [14–16]. Collectively, these pathogen-induced mechanisms—often synergistic with oxidative stress—drive the initiation and progression of various cutaneous pathologies.

Research on the anti-inflammatory and antimicrobial properties of NBPs has primarily aimed at mitigating symptoms induced by inflammation and microbial infections. To date, most studies have focused on individual extracts, leaving the potential benefits of combining promising NBP candidates largely unexplored. Addressing this gap, the present study systematically evaluated NBPs, selected the most effective candidates, and examined a composite extract derived from them to assess its potential as a novel functional ingredient.

2. Materials and Methods

2.1. Bioactivity Assay Materials

2,2-diphenyl-1-picrylhydrazyl (DPPH), 2,2-azino-bis(3-ethylbenzthiazoline-6-sulfonic acid) diammonium salt (ABTS), butylated hydroxyanisole (BHA), potassium persulfate, trizma base, Elastase from porcine pancreas, Type I, N-Succinyl-Ala-Ala-Ala-p-nitroanilide, ursolic acid (UA), L-3,4-dihydroxyphenylalanine (L-DOPA) and tyrosinase from mushroom were purchased from Sigma-Aldrich (St. Louis, MO, USA). Ascorbic acid (AA) was purchased from Duchefa Biochemie (Haarlem, Netherlands). Sodium carbonate anhydrous (Na_2CO_3) and sodium hydroxide (NaOH) were purchased from DAEJUNG (Siheung, Republic of Korea). Diethylene glycol and dimethyl sulfoxide (DMSO) were purchased from Junsei Chemical Co., Ltd. (Tokyo, Japan). Sodium phosphate was purchased from SAMCHUN (Pyeongtaek, Republic of Korea).

2.2. Cell Culture and Experimental Material

Lipopolysaccharide (LPS), Griess reagent were purchased from Sigma-Aldrich (St. Louis, MO, USA). 3-(4,5-Dimethylthiazol-2-yl)-2,5-diphenyltetrazolium bromide (MTT) was purchased from Duchefa Biochemie (Haarlem, The Netherlands). The murine

macrophage cell line RAW 264.7 was obtained from the American Type Culture Collection (ATCC, Manassas, VA, USA). Cells were cultured in Dulbecco's Modified Eagle's Medium (DMEM; Capricorn Scientific GmbH, Ebsdorfergrund, Germany) supplemented with 10% fetal bovine serum (FBS) and 1% penicillin/streptomycin (Capricorn Scientific GmbH) at 37 °C in a humidified incubator containing 5% CO_2 (PHCbi, Tokyo, Japan). To avoid DMSO-induced artifacts, the final concentration was kept below 0.5%.

2.3. Plant and Fruit Materials

Plant and fruit materials used in this study included peanut (*Arachis hypogaea* L., *A. hypogaea*), apple (*Malus pumila* Mill., *M. pumila*), asian pear (*Pyrus pyrifolia* var. *cultiva* (Makino) Nakai, *P. pyrifolia*), brown seaweed (*Saccharina japonica* (Areschoug) C.E. Lane, C. Mayes, Druehl & G.W. Saunders, *S. japonica*), onion (*Allium cepa* L., *A. cepa*), purple corn (*Zea mays* L., *Z. mays*), bur cucumber (*Sicyos angulatus* L., *S. angulatus*), and hinoki cypress (*Chamaecyparis obtusa* (Siebold & Zucc.) Endl., *C. obtusa*). *A. hypogaea* was cultivated in Gumi, Gyeongsangbuk-do, and separated into roots, stems, kernels, and shells. *M. pumila* and *P. pyrifolia* were purchased from Geochang, Gyeongsangnam-do, and Ulju, Ulsan, respectively, and the pomace remaining after juice extraction was used. *S. japonica* was collected from Gijang, Busan. *A. cepa* was obtained from onions grown in Changnyeong, Gyeongsangnam-do, and the outer peels were separated for use. *Z. mays* purple corn was cultivated in Gochang, Jeonbuk-do, and the cobs and husks were separated. *S. angulatus* was collected from Chungju, Chungcheongbuk-do, and *C. obtusa* roots were obtained from cultivated trees in Dalseong, Daegu, and used in the study. All plant materials were botanically authenticated at the species level using the Species Korea database operated by the National Institute of Biological Resources under the Ministry of Environment of the Republic of Korea (https://species.nibr.go.kr, accessed on 29 November 2025). The scientific names of all plant materials were verified based on the officially registered nomenclature in this database to minimize potential errors in taxonomic identification.

2.4. Extraction Process

Raw materials were extracted using 95% ethanol, diluted with triple-distilled water to achieve final concentrations of either 30% or 70%. For each extraction, 20 g of raw material was combined with 180 g of solvent, maintaining a 1:9 (*w*/*w*) ratio. The mixture was filtered through filter paper during each extraction cycle to remove insoluble impurities, and the filtrations were collected and stored. For *Z. mays* (cob and husk), the raw materials were pre-frozen and lyophilized prior to extraction, which was conducted three times for 24 h each using 30% ethanol. For all other materials—*A. hypogaea* (kernel, shell, leaf/stem, root), *A. cepa* (peel), *M. pumila* (pomace), *P. pyrifolia* (pomace), *S. japonica* (discarded thallus), *S. angulatus* (whole plant), and *C. obtusa* (root)—extractions were performed three times for 24 h each using 70% ethanol. All extracts were subsequently concentrated under reduced pressure at 60 °C using a rotary evaporator (HAHNSHIN S&T Co. Ltd., Gyeonggi-do, Republic of Korea) and then lyophilized to yield the final extracts, which were used for downstream experiments.

2.5. Total Flavonoid Content Analysis

Total flavonoid content was determined using a colorimetric assay. Briefly, 50 µL of sample solution was mixed with 500 µL of diethylene glycol and 500 µL of 1 N NaOH. The mixture was incubated at 37 °C for 1 h in an incubator (PHCbi, Tokyo, Japan). After incubation, the absorbance was measured at 420 nm using a microplate reader (BioTek Instruments, Winooski, VT, USA). The total flavonoid content was calculated based on a calibration curve constructed using quercetin as a standard ($R^2 > 0.99$).

2.6. Total Polyphenol Content Analysis

Total polyphenol content was measured using the Folin–Ciocalteu method. Briefly, 50 µL of sample solution was mixed with 50 µL of Folin–Ciocalteu reagent and incubated at room temperature in the dark for 5 min. Subsequently, 50 µL of 10% Na_2CO_3 solution was added, and the mixture was further incubated at room temperature in the dark for 1 h. The absorbance was measured at 640 nm using a microplate reader (BioTek Instruments). The total polyphenol content was calculated using a calibration curve prepared with tannic acid as a standard ($R^2 > 0.98$).

2.7. DPPH Radical Scavenging Activity

100 µL of samples were treated with 50 µL of 0.2 mM DPPH solution. BHA was used as a positive control. The plate was incubated in the dark at room temperature for 30 min, and the absorbance was measured spectrophotometrically at 517 nm using a microplate reader (BioTek Instruments) [17].

2.8. $ABTS^+$ Radical Scavenging Activity

The $ABTS^+$ radical solution was generated by mixing 7.4 mM $ABTS^+$ with an equal volume of 2.6 mM potassium persulfate, followed by incubation in the dark at room temperature for 24 h. 100 µL of samples were subsequently treated with 100 µL of the prepared $ABTS^+$ radical solution, with BHA included as a positive control. After 7 min of incubation in the dark at room temperature, the absorbance was measured spectrophotometrically at 734 nm using a microplate reader (BioTek Instruments) [18].

2.9. Tyrosinase Inhibitory Activity

40 µL of samples were treated with 80 µL of 67 mM sodium phosphate buffer, pH 6.8, followed by 40 µL of tyrosinase, 125 units. The reaction was initiated by adding 40 µL of 25 mM L-DOPA. AA was used as a positive control. A solvent control was included using DMSO at the same concentration as in the sample-treated groups. The plate was incubated in the dark at 37 °C for 30 min, and the absorbance was measured spectrophotometrically at 420 nm using a microplate reader (BioTek Instruments) [19].

2.10. Elastase Inhibitory Activity

100 µL of samples were treated with 50 µL of 0.4 mM Tris-HCl buffer, pH 8.6, followed by 50 µL of elastase at 1.2 units/mL, prepared in 0.05 mM Tris-HCl buffer. The plate was incubated in the dark at 37 °C for 30 min. Subsequently, 100 µL of 10,000 µg/mL N-Succinyl-Ala-Ala-Ala-p-nitroanilide, also prepared in 0.05 mM Tris-HCl buffer, was added to each well and allowed to react in the dark at room temperature for 20 min. UA was used as the positive control. A solvent control was included using DMSO at the same concentration as in the sample-treated groups. The absorbance was measured spectrophotometrically at 405 nm using a microplate reader (BioTek Instruments) [20].

2.11. Cell Viability Assay

RAW 264.7 cells were seeded into 96-well plates and treated with samples. The cells were incubated at 37 °C in a humidified incubator (PHCbi) with 5% CO_2 for 24 h. After incubation, the culture medium was removed, and 100 µL of MTT solution was added. The plate was incubated in the dark at 37 °C for 1 h. Following removal of the MTT solution, 100 µL of DMSO was added to dissolve the purple formazan crystals, and final concentration of DMSO was kept constant across all treatment and control groups. and the absorbance was measured at 570 nm using a microplate reader (BioTek Instruments) [21].

2.12. Nitric Oxide (NO) Production Assay

RAW 264.7 cells were seeded into 6-well plates and treated with samples for 2 h. Subsequently, 200 ng/mL LPS was added based on previously validated experimental conditions in RAW 264.7 macrophages, and the cells were incubated at 37 °C in a CO_2 incubator (PHCbio) for 16 h. Then, 100 µL of culture supernatants were mixed with an equal volume of Griess reagent in a 96-well plate. Nitric oxide production was determined by measuring the absorbance at 540 nm using a microplate reader (BioTek Instruments) [22–24].

2.13. Western Blotting

After sample treatment, RAW 264.7 cells were washed with phosphate-buffered saline (PBS) at room temperature. Cells were lysed on ice for 10 min in lysis buffer containing protease and phosphatase inhibitors, with the process repeated three times. Lysates were centrifuged at 12,000 rpm for 10 min at 4 °C, and protein concentrations in the supernatant were quantified using Bradford reagent (Bio-Rad, Hercules, CA, USA). iNOS was obtained from Invitrogen (Carlsbad, CA, USA), and COX-2 was obtained from Cell Signaling Technology (Danvers, MA, USA), Anti β-actin Rabbit (β-actin) from Abbkine (Wuhan, China). Equal amounts of protein were separated on 8% SDS-PAGE gels and transferred to nitrocellulose membranes (GE Healthcare Life Sciences, Marlborough, MA, USA). Membranes were blocked with 5% skim milk at room temperature for 1 h, followed by overnight incubation at 4 °C with primary antibodies diluted 1:1000. The membranes were then incubated for 2 h with horseradish peroxidase (HRP)-conjugated secondary antibodies diluted 1:10,000. Protein bands were visualized using enhanced chemiluminescence (Abbkine, Wuhan, China) [25]. The uncropped immunoblot images are provided in Figure S1.

2.14. Kirby-Bauer Assay

Bacterial strains were cultured in liquid media under appropriate growth conditions. *P. aeruginosa*, *E. coli*, *S. aureus*, *C. acnes*, *C. albicans* and *G. vaginalis* were used. *C. acnes* and *G. vaginalis* was incubated at 37 °C in a CO_2 incubator (ASTEC Korea Co., Ltd., Seoul, Republic of Korea), while *P. aeruginosa*, *E. coli*, *S. aureus*, and *C. albicans* were cultured at 37 °C in a standard incubator (Duri Science Inc., Bucheon, Republic of Korea). 100 µL of cultured bacteria were spread uniformly on solid media using sterile swabs. Sterilized 8 mm paper disks (ADVANTEC, Tokyo, Japan) were placed on the inoculated plates, and samples were applied to the disks. 5% methyl paraben (MP) was used as a positive control, and DMSO served as a negative control. After overnight incubation, the diameter of the clear zones surrounding each disk was measured to evaluate antibacterial activity [26].

2.15. Selection Criteria and Scoring System for NBPs

Evaluation To identify NBP samples with superior functional potential, a quantitative scoring system was established and applied across five assay categories: antioxidant, tyrosinase inhibition, elastase inhibition, antimicrobial, and anti-inflammatory activities. Selection was based on the relative performance of all samples within each category. In the general scoring framework, the top-performing extract in each assay, as well as any extract exhibiting at least 90% of the activity of the positive control, was assigned 3 points. The second-ranked extract received 2 points, and the third-ranked extract received 1 point. This approach enabled a normalized comparison of bioactivity across assays with differing experimental scales. For antimicrobial activity, scoring was determined by the number of microbial strains inhibited. Extracts that inhibited all six tested strains received 3 points, those inhibiting five strains received 2 points, and those inhibiting four or three strains received 1 point. In addition, the top three extracts were awarded 1 supplementary point

each based on the magnitude of inhibition to further differentiate antimicrobial efficacy. For anti-inflammatory activity, the three extracts demonstrating the strongest inhibition of nitric oxide production in LPS-stimulated RAW 264.7 macrophages were each given an additional 2 points to emphasize performance in this biologically critical category.

2.16. Selection Criteria and Heatmap-Based Visualization of NBPs

To comparatively visualize the multifunctional screening results, the functional performance of NBPs across five biological categories—antioxidant, tyrosinase inhibition, elastase inhibition, antimicrobial, and anti-inflammatory activities—was visualized using a heatmap after calculating z-score. All analyses and visualizations were performed using Microsoft Excel software (Microsoft Corp., Redmond, WA, USA).

2.17. High-Performance Liquid Chromatography (HPLC) Fingerprint Analysis

The extract samples were dissolved in methanol to a final concentration of 100 mg/mL and filtered through a 0.22 μm syringe filter prior to analysis. HPLC analysis was performed using a YMC-Pack Pro C18 column (4.6 × 150 mm, 3 μm, Agilent Technologies, Santa Clara, CA, USA). The column temperature was maintained at 30 °C. The mobile phase consisted of solvent A (0.1% trifluoroacetic acid in deionized water) and solvent B (methanol), with a gradient elution as follows: 0–5 min, 55% A; 20 min, 25% A; 25 min, 20% A; 30 min, 10% A; 30.1–37.0 min, 0% A; 37.1–47.0 min, 55% A. The flow rate was set at 0.6 mL/min. Detection was carried out using a UV-Vis detector (Agilent Technologies, Santa Clara, CA, USA) at 370 nm, and a sample volume of 10 μL was injected. Detailed chromatographic conditions are provided in Table S1. The HPLC chromatograms of the selected samples (A. *hypogaea* shell, *C. obtusa* root, *A. cepa* peel, and *S. angulatus* whole plant) are presented in Figure S2.

2.18. Statistical Analysis

All experiments were independently performed in triplicate under identical conditions. The resulting data are presented as the mean ± standard deviation (SD). Statistical analyses were carried out using Microsoft Excel 2016 (Microsoft Corp., Redmond, WA, USA). Differences between treatment groups were evaluated using an unpaired, two-tailed Student's *t*-test, and statistical significance was defined as $p < 0.05$. Significance levels were denoted as * $p < 0.05$, ** $p < 0.01$, and *** $p < 0.001$.

3. Results

3.1. Extraction Yield of NBPs

NBPs were separated by part and pre-processed prior to extraction. The fractions were extracted following the protocol shown in Figure 1, and the extraction yields were measured and summarized in Table 1. The extraction yield was calculated using the formula: freeze-dried extract weight divided by the initial raw material weight, multiplied by 100%. Among the samples, *M. pumila* (pomace) extract demonstrated the highest extraction yield at 60.71%, followed by *P. pyrifolia* (pomace) at 47.55% and *S. japonica* (discarded thallus) at 23.90%. In contrast, the lowest extraction yields were observed for *A. hypogaea* (shell) at 2.11%, *Z. mays* (husk) at 2.30%, and *A. cepa* (peel) at 2.72%.

Table 1. Extraction yield of NBPs.

A. hypogaea (kernel)	*A. hypogaea* (shell)	*A. hypogaea* (leaf/stem),	*A. hypogaea* (root)	*A. cepa* (peel)	*M. pumila* (pomace)
6.39%	2.11%	9.83%	2.72%	8.83%	60.71%

Table 1. *Cont.*

P. pyrifolia (pomace)	*S. japonica* (discarded thallus)	*Z. mays* (cob)	*Z. mays* (husk)	*S. angulatus* (whole plant)	*C. obtusa* (root)
47.55%	23.90%	3.28%	2.30%	6.04%	6.40%

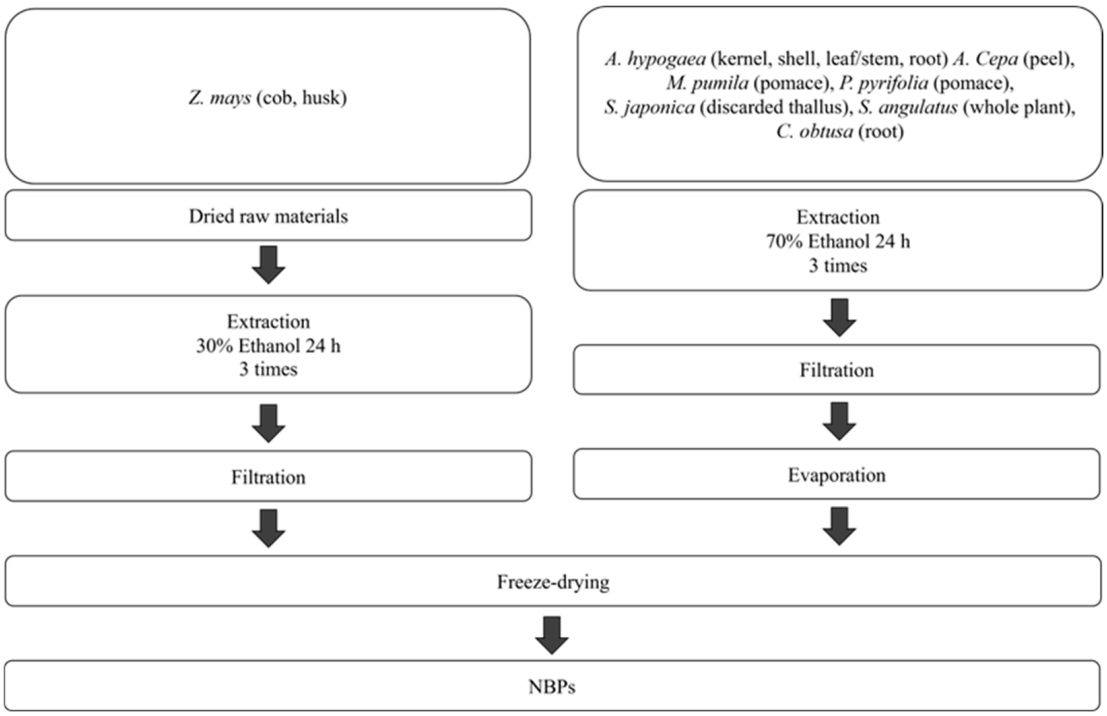


Figure 1. Extraction process of NBPs.

3.2. Comparative Analysis of Phytochemical Contents and Biological Activities of NBPs

Prior to the evaluation of the biofunctional activities of the NBP extracts, preliminary phytochemical analysis was conducted. The results showed that *A. cepa* (peel), *Z. mays* (cob), and *Z. mays* (husk) contained relatively high levels of total polyphenols and flavonoids (Figure 2A,B). Subsequently, NBP extracts were diluted to a final concentration of 100 μg/mL and comparatively evaluated for their antioxidant, tyrosinase inhibition, and elastase inhibition activities. NBP extracts were diluted to a final concentration of 100 μg/mL and comparatively evaluated for their antioxidant, tyrosinase inhibition, and elastase inhibition activities. All extracts and the positive control were treated at a final concentration of 100 μg/mL, a condition widely used in previous studies for initial screening of natural product bioactivity [27,28]. Comprehensive assessment of DPPH and $ABTS^+$ radical-scavenging activities revealed that *A. cepa* (peel), *Z. mays* (cob), *Z. mays* (husk), and *C. obtusa* (root) exhibited the highest antioxidant capacities, while *A. hypogaea* (kernel) and *A. hypogaea* (shell) showed the second highest activity (Figure 2C,D). BHA was used as a positive control, as it is a well-established phenolic antioxidant with clearly demonstrated efficacy. Moreover, BHA exhibits high reproducibility and stability in chemical antioxidant assays, making it a suitable reference compound for the present study [29]. Tyrosinase inhibition activity was assessed via a mushroom tyrosinase inhibition assay, with *A. cepa* (peel) demonstrating the strongest inhibitory effect, followed by *C. obtusa* (root), whereas the remaining extracts exhibited negligible activity (Figure 2E). Elastase inhibition activity was evaluated through an elastase inhibition assay, and *C. obtusa* (root) displayed the

strongest inhibitory effect, followed by *A. hypogaea* (shell), while the other extracts showed no significant inhibition (Figure 2F).

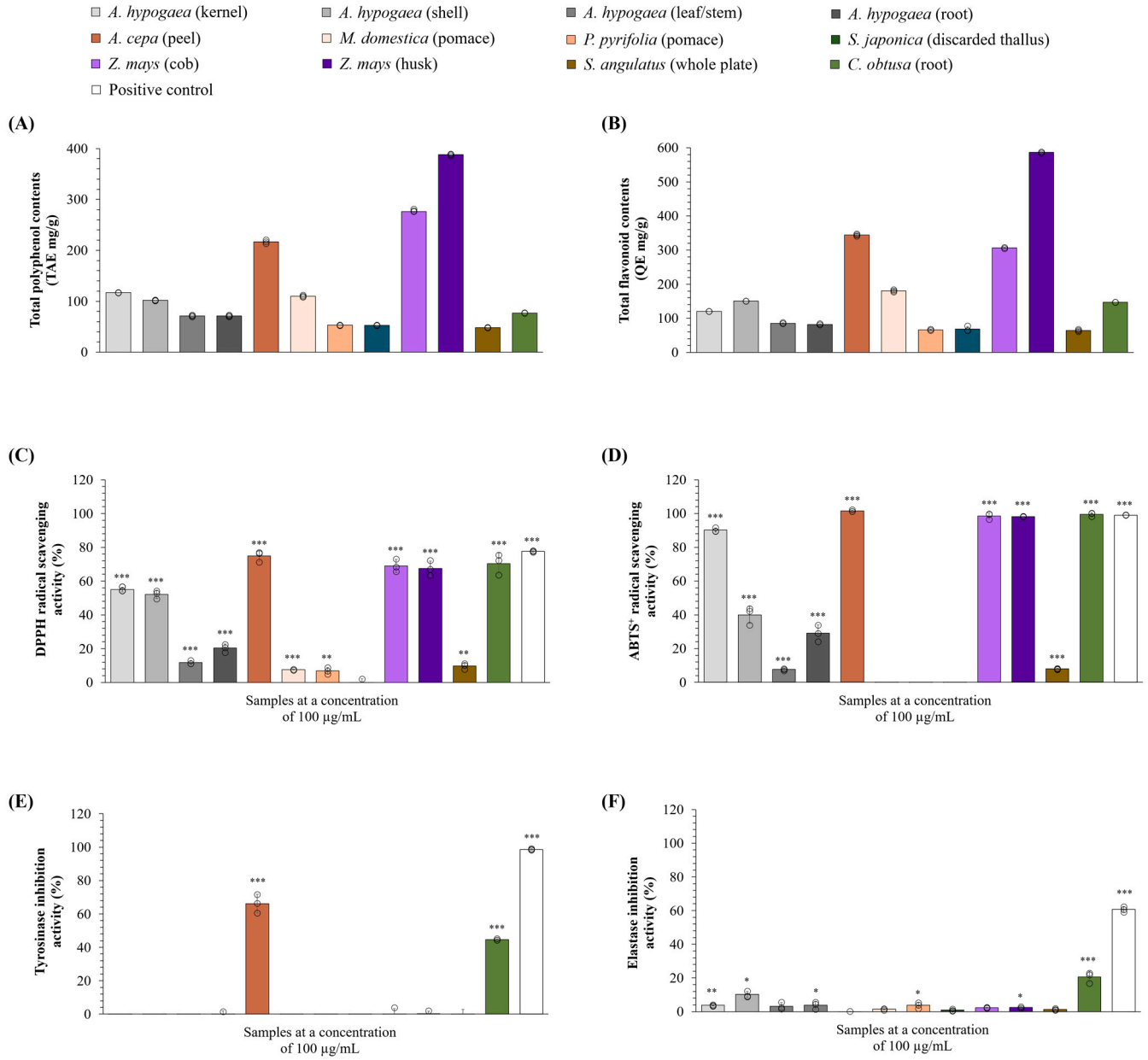


Figure 2. Comparative analysis of phytochemical contents and biological activities of NBPs. (**A**): Total polyphenol contents (TAE, tannic acid equivalents); (**B**): Total flavonoid contents (QE, quercetin equivalents); (**C**): DPPH radical scavenging activity; (**D**): ABTS$^+$ radical scavenging activity; (**E**): Mushroom tyrosinase inhibition activity; (**F**): Elastase inhibition activity; Positive control; BHA: Butylated hydroxy anisole (**C**,**D**), AA: Ascorbic acid (**E**), UA: Ursolic acid (**F**). The statistical analysis of all data was performed using Microsoft Excel software. Data represents the mean ± standard deviation (SD), $n = 3$. * $p < 0.05$, ** $p < 0.01$, *** $p < 0.001$ compared with untreated control. Each circle represents an individual data point from independent samples.

3.3. Comparative Antimicrobial Activity of NBPs

The antimicrobial efficacy of NBPs against six microorganisms associated with skin diseases and inflammation was evaluated using the paper disk diffusion method. Each extract was applied at a 5% concentration, and the diameter of the inhibition zones (clear zones) was measured (Figures 3 and 4). Among the extracts, *A. cepa* (peel) exhibited the strongest activity against all six tested strains. *C. obtusa* (root) showed clear inhibition

against five strains, excluding *G. vaginalis*. *A. hypogaea* (shell and root) inhibited four strains, excluding *G. vaginalis* and *C. albicans*. *S. angulatus* (whole plant) demonstrated antimicrobial effects against all strains except *E. coli*, *C. albicans*, and *G. vaginalis*.

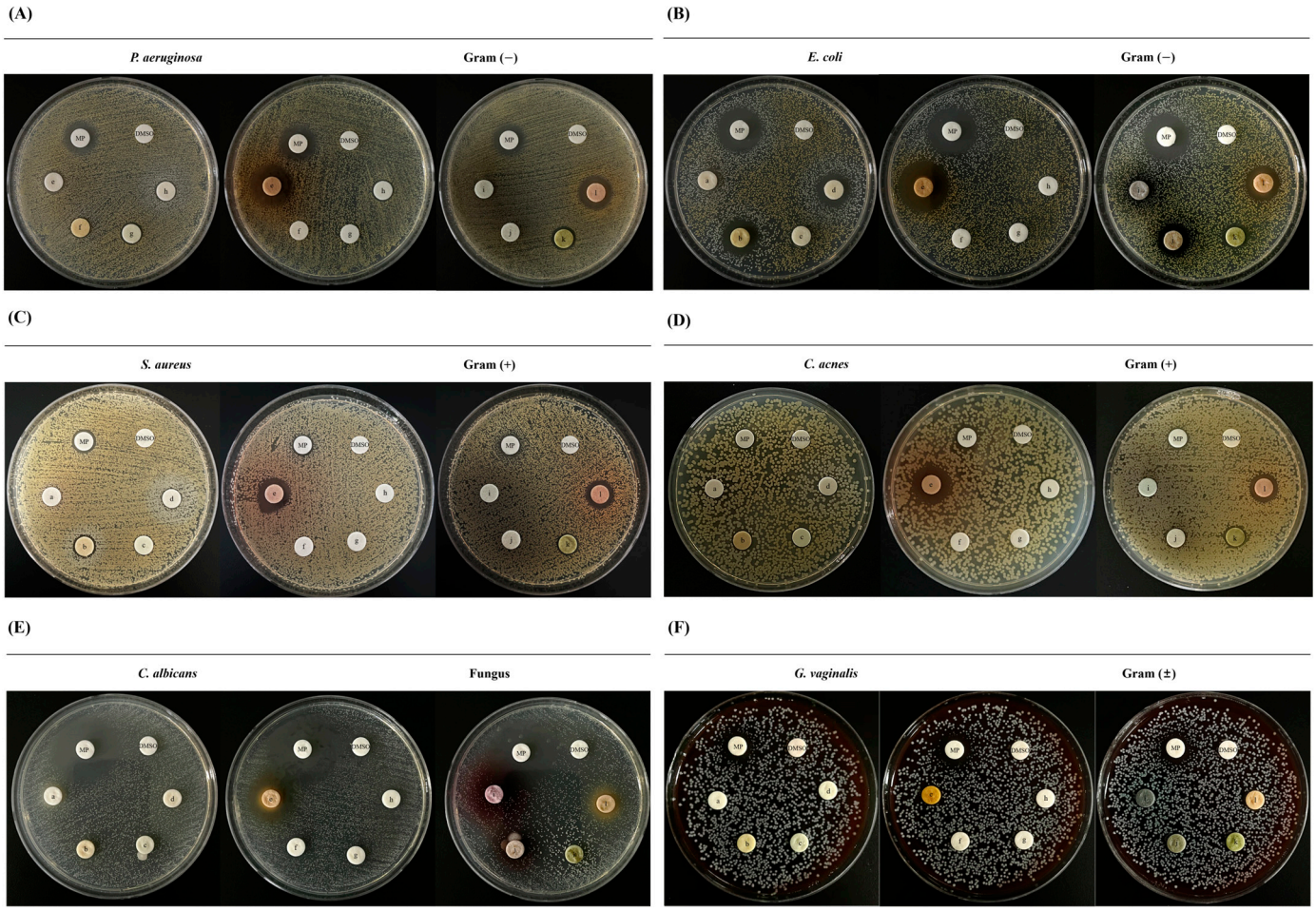


Figure 3. Antimicrobial activity of NBPs. Positive control: methyl paraben (MP), negative control: dimethyl sulfoxide (DMSO). Paper disk size: 8 mm. (**A**) *P. aeruginosa*; (**B**) *E. coli*; (**C**) *S. aureus*; (**D**) *C. acnes*; (**E**) *C. albicans*; (**F**) *G. vaginalis*. a: *A. hypogaea* (kernel), b: *A. hypogaea* (shell) c: *A. hypogaea* (leaf/stem), d: *A. hypogaea* (root), e: *A. cepa* (peel), f: *M. pumila* (pomace), g: *P. pyrifolia* (pomace), h: *S. japonica* (discarded thallus) i: *Z. mays* (cob), j: *Z. mays* (husk), k: *S. angulatus* (whole plant), l: *C. obtusa* (root).

3.4. Anti-Inflammatory Activity of NBPs

NO production was quantified in LPS-stimulated RAW 264.7 cells, a murine macrophage line widely used for assessing inflammatory responses. The anti-inflammatory potential of the NBPs was evaluated at two concentrations, 10 μg/mL and 100 μg/mL, to determine their efficacy in modulating NO production. At the lower concentration of 10 μg/mL, none of the extracts significantly inhibited NO production compared with the untreated control, suggesting that this dose was largely ineffective in suppressing the inflammatory response (Figure 5A). At 100 μg/mL, however, the extracts displayed markedly different levels of activity. *S. angulatus* (whole plant), *C. obtusa* (root), and *A. cepa* (peel) exhibited the strongest inhibitory effects on NO production (Figure 5B). Notably, *S. angulatus* and *C. obtusa* reduced NO production to 9.31% and 11.72% of the LPS-treated group (100%), approaching the untreated control level (9.09%).

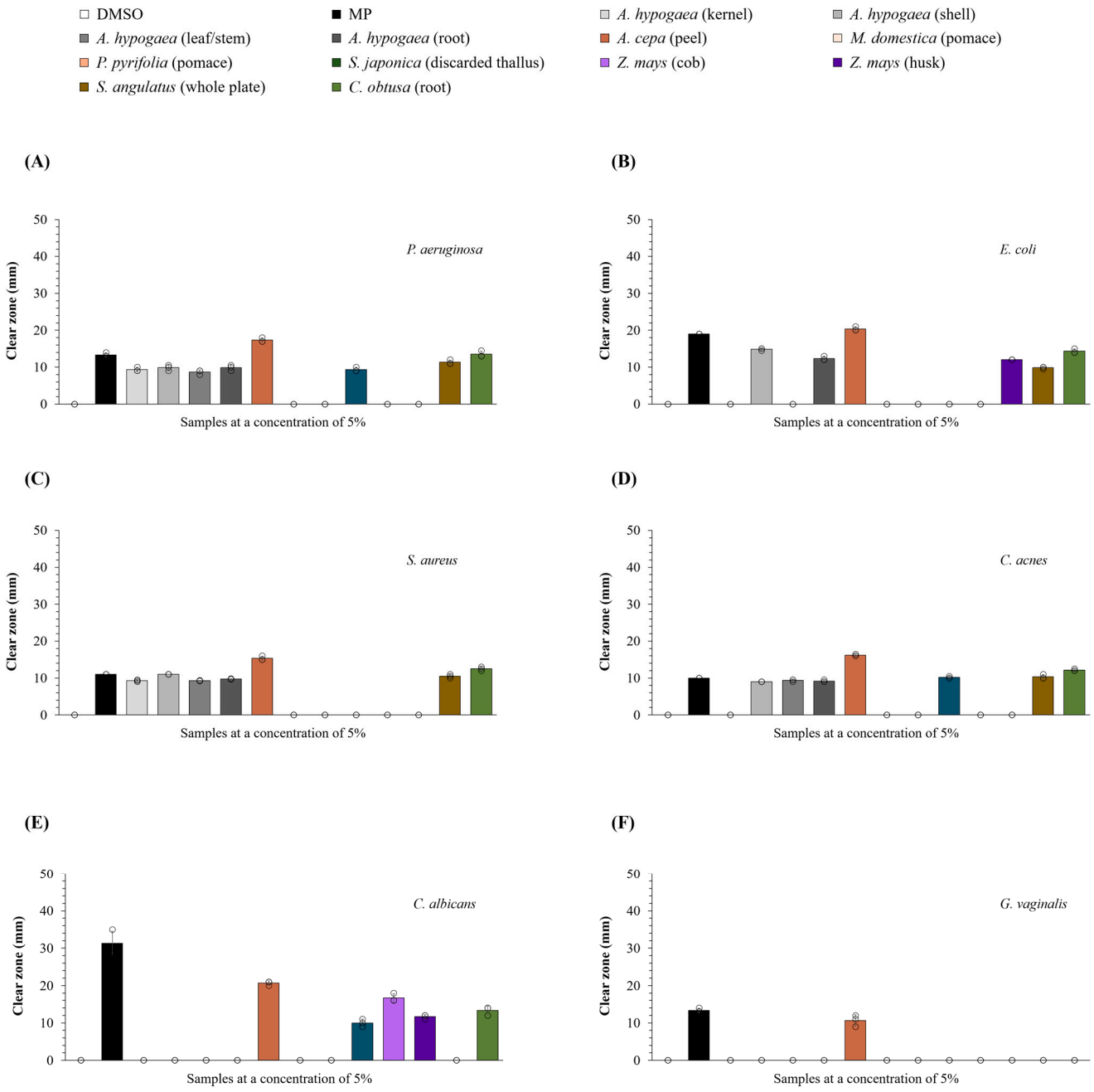


Figure 4. Clear zones represent the antimicrobial activity of NBPs. Positive control: methyl paraben (MP), negative control: dimethyl sulfoxide (DMSO). Paper disk size: 8 mm. (**A**) *P. aeruginosa*; (**B**) *E. coli*; (**C**) *S. aureus*; (**D**) *C. acnes*; (**E**) *C. albicans*; (**F**) *G. vaginalis*. Each circle represents an individual data point from independent samples.

3.5. Comprehensive Evaluation and Selection of NBPs

A multi-criteria scoring system integrating five functional activities, including antioxidant activity, tyrosinase inhibition, elastase inhibition, antimicrobial activity, and anti-inflammatory activity, was applied to comparatively evaluate all NBPs (Figure 6). Based on cumulative scores, four extracts with the highest overall functional performance were identified as the most promising candidates. To assess their combined potential across multiple bioactivities, particularly anti-inflammatory effects, *C. obtusa* (root) achieved the highest total score of 13, followed by *A. cepa* (peel) with 11, *A. hypogaea* (shell) with 5, and *S. angulatus* (whole plant) with 4. Lower-ranked samples were *Z. mays* (cob) and *Z. mays* (husk) with 3, *A. hypogaea* (kernel) with 2, *A. hypogaea* (root) with 1, and other extracts with

0. Figure 6 presents a heat map and corresponding graph based on this scoring system, visually highlighting that the top four extracts, *A. cepa* (peel), *C. obtusa* (root), *A. hypogaea* (shell), and *S. angulatus* (whole plant), were selected for combination into the NBPs complex. The HPLC fingerprint profiles of the four selected extracts were additionally confirmed and are presented in Figure S2.

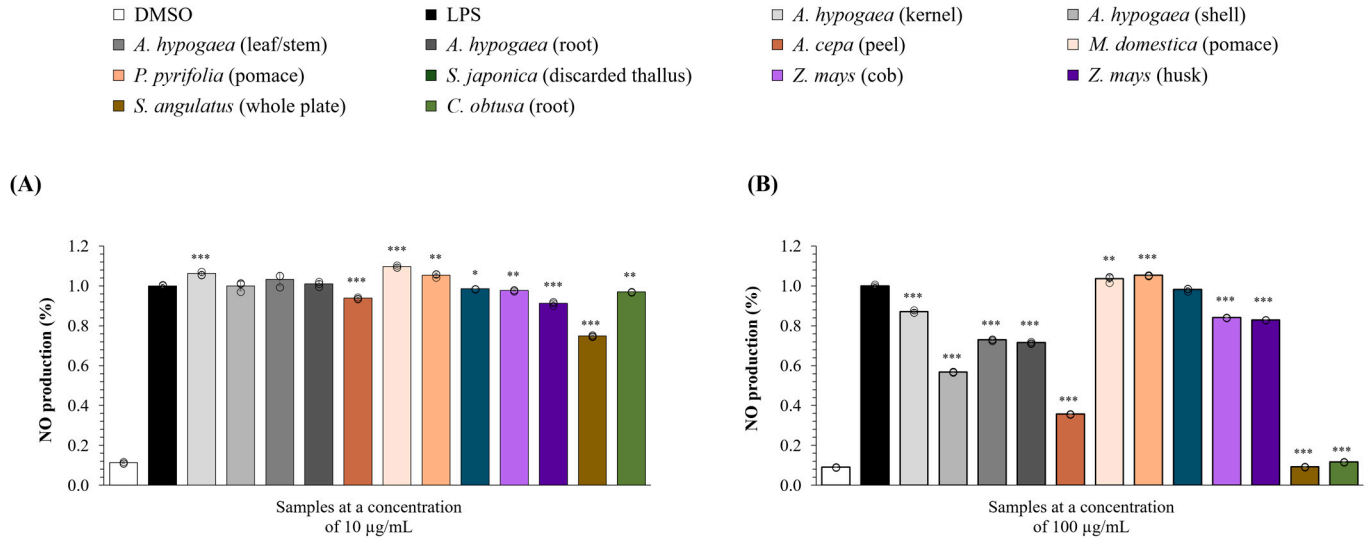


Figure 5. Anti-inflammatory effect of NBPs. Inhibitory effects of NBPs on NO production in LPS-stimulated RAW 264.7 cells, as assessed through the Griess reagent assay. (**A**): NO inhibition at 10 μg/mL NBPs. (**B**): NO production at 100 μg/mL NBPs. RAW 264.7 were treated for 2 h prior to LPS stimulation and subsequently incubated for an additional 16 h. The statistical analysis of all data was performed using Microsoft Excel software. Data represents the mean ± standard deviation (SD), $n = 3$. * $p < 0.05$, ** $p < 0.01$, *** $p < 0.001$ compared with LPS stimulated group. Each circle represents an individual data point from independent samples.

3.6. Cytotoxicity of Four Selected NBPs

Prior to the experiments, the cytotoxicity of each extract was evaluated in RAW 264.7 macrophages to identify non-cytotoxic ranges and determine suitable mixing proportions. Concentrations that maintained cell viability above 90% were selected as reference concentrations. Based on these results, the maximum non-cytotoxic levels were determined to be 100 μg/mL for *A. hypogaea* (shell), 50 μg/mL for *S. angulatus* (whole plant), 25 μg/mL for *A. cepa* (peel), and 12.5 μg/mL for *C. obtusa* (root) (Figure 7). These concentrations were subsequently used to establish the 8:4:2:1 ratio for the NBP complex.

3.7. Biofunctional and Anti-Inflammatory Evaluation of NBP Complex

The biological functions and anti-inflammatory activities of the NBP complex were evaluated through antioxidant, tyrosinase inhibition, elastase inhibition, cytotoxicity, and inflammatory mediator assays. Antioxidant assessment revealed marked activity in the DPPH radical scavenging assay at 200 μg/mL and in the ABTS radical scavenging assay at 100 μg/mL, both exhibiting inhibition rates exceeding 95% (Figure 8A,B). Tyrosinase inhibition activity was minimal (Figure 8C), whereas the elastase inhibition assay showed a 13.80% inhibition at 200 μg/mL (Figure 8D). Based on the preliminary cell viability data obtained from Figure 7, the maximum treatment concentration for the present experiment was set at 750 μg/mL. Under these conditions, cell viability remained above 90% at 187.5 μg/mL (Figure 8E). Building on this, nitric oxide production was measured at 50 and 100 μg/mL, with the NBP complex reducing LPS-induced NO levels by 18.96% and 12.12%, respectively (Figure 8F). Western blot analysis further demonstrated that the

expression of the inflammatory mediators iNOS and COX-2 decreased in a dose-dependent manner at both concentrations (Figure 8G), supporting the anti-inflammatory properties of the NBP complex.

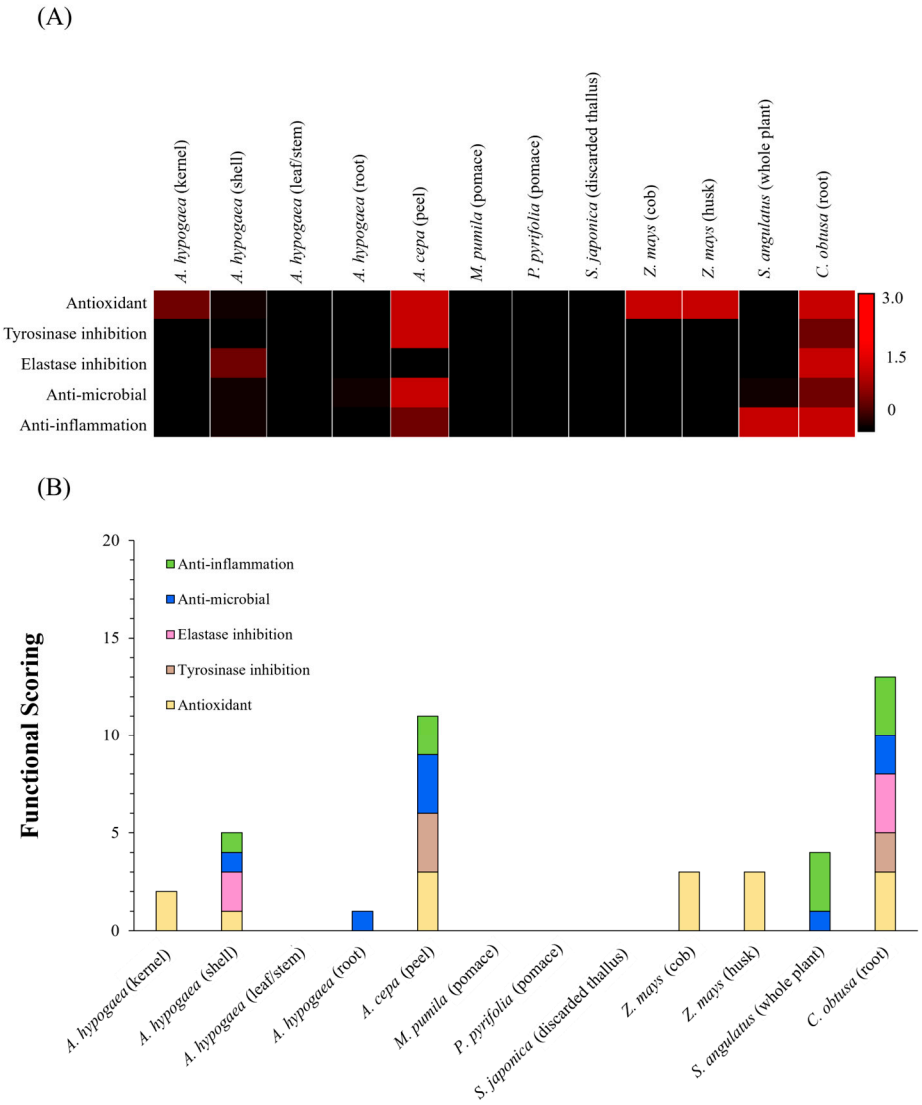


Figure 6. Overall Functional Assessment of NBPs: cumulative functional performance across antioxidant, tyrosinase inhibition, elastase inhibition, antimicrobial, and anti-inflammatory activities. (**A**): Heatmap showing relative performance within each functional category. (**B**): Cumulative scores calculated based on relative performance within each category. All data processing and visualization were performed using Microsoft Excel software.

3.8. Antimicrobial Properties of the NBP Complex

The antimicrobial activity of the NBP complex was evaluated against six microbial strains (Figure 9). The complex exhibited inhibitory effects against all tested microorganisms except *G. vaginalis*. At 1% concentration, the NBP complex showed antimicrobial activity against *P. aeruginosa*, *E. coli*, *C. acnes*, and *C. albicans*. At concentrations of 3% and 5%, inhibitory effects additionally extended to *S. aureus*, resulting in concentration-dependent antimicrobial activity across five strains. These results indicate that the NBP complex possesses antimicrobial activity against several skin-associated pathogenic or inflammation-exacerbating microorganisms, except for *G. vaginalis*.

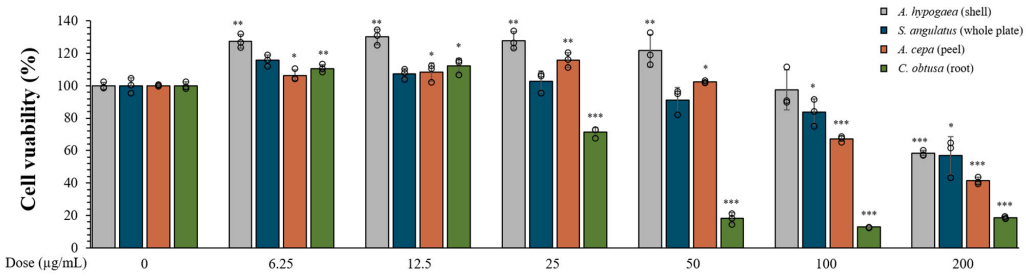


Figure 7. Cytotoxicity of Four Selected NBPs in RAW 264.7 Cells. RAW 264.7 cell were seeded in 96 well plates and treated with *A. hypogaea* (shell), *S. angulatus* (whole plant), *A. cepa* (peel), and *C. obtusa* (root) for 24 h. Cell viability was determined by MTT assay. All statistical analyses were conducted with Microsoft Excel software. Data represents the mean ± SD, $n = 3$. * $p < 0.05$, ** $p < 0.01$, *** $p < 0.001$ in comparison to non-treated groups. Each circle represents an individual data point from independent samples.

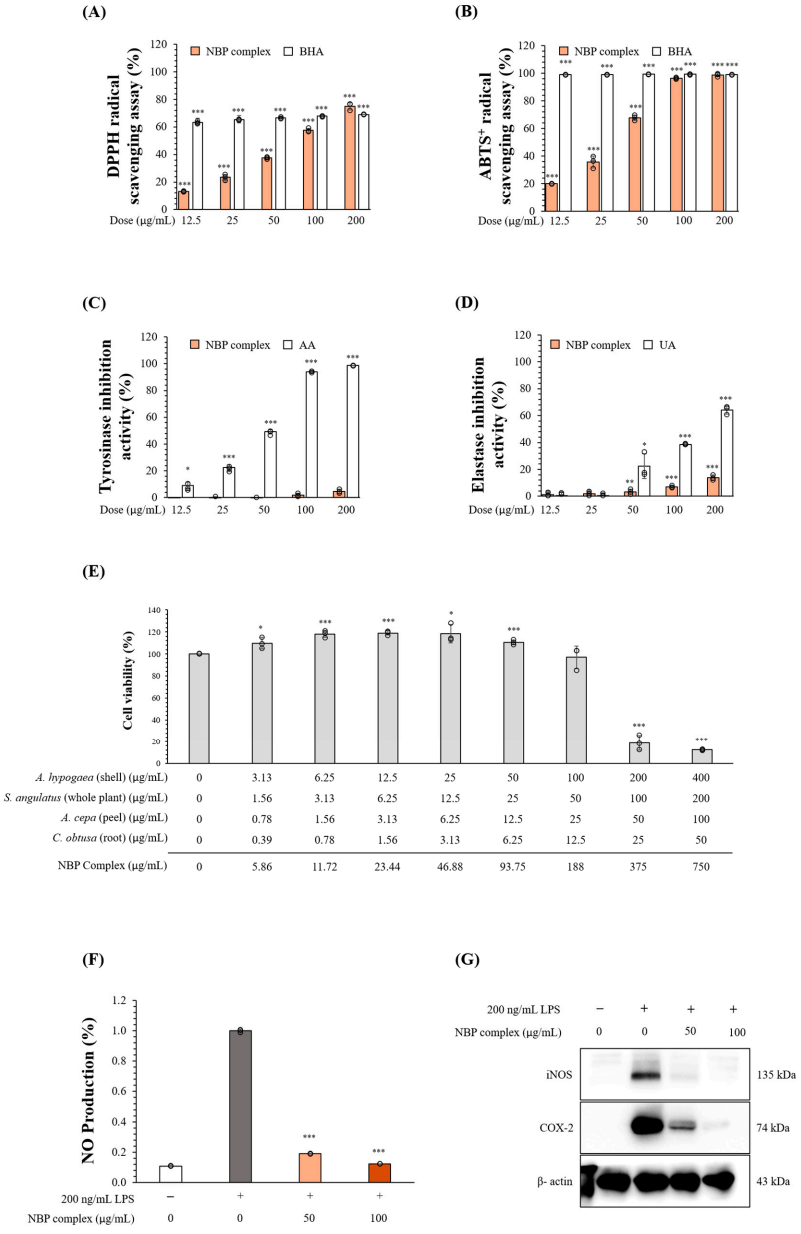


Figure 8. In vitro Activities of NBP Complex. The NBP complex, composed of *A. hypogaea* (shell), *S. angulatus* (whole plant), *A. cepa* (peel), and *C. obtusa* (root), was evaluated for its diverse functional properties at in vitro. (**A**): DPPH radical scavenging activity. (**B**): ABTS$^+$ radical scavenging activity.

(**C**): Mushroom tyrosinase inhibitory activity. (**D**): Elastase inhibition activity. (**E**): Cell viability in RAW 264.7 cells following 24 h treatment with the NBP complex. (**F**): Inhibitory effects on NO production in LPS-stimulated RAW 264.7 cells, assessed using the Griess reagent assay. (**G**): Effects on iNOS and COX-2 expression in LPS-stimulated RAW 264.7 cells. The complete Western blot images are provided in Figure S1. RAW 264.7 cells were pretreated with the NBP complex for 2 h prior to LPS stimulation and subsequently incubated for an additional 16 h (**F**,**G**). All statistical analyses were conducted with Microsoft Excel software. Data represents the mean ± SD, $n = 3$. * $p < 0.05$, ** $p < 0.01$, *** $p < 0.001$ compared with untreated control or LPS-only group. Each circle represents an individual data point from independent samples.

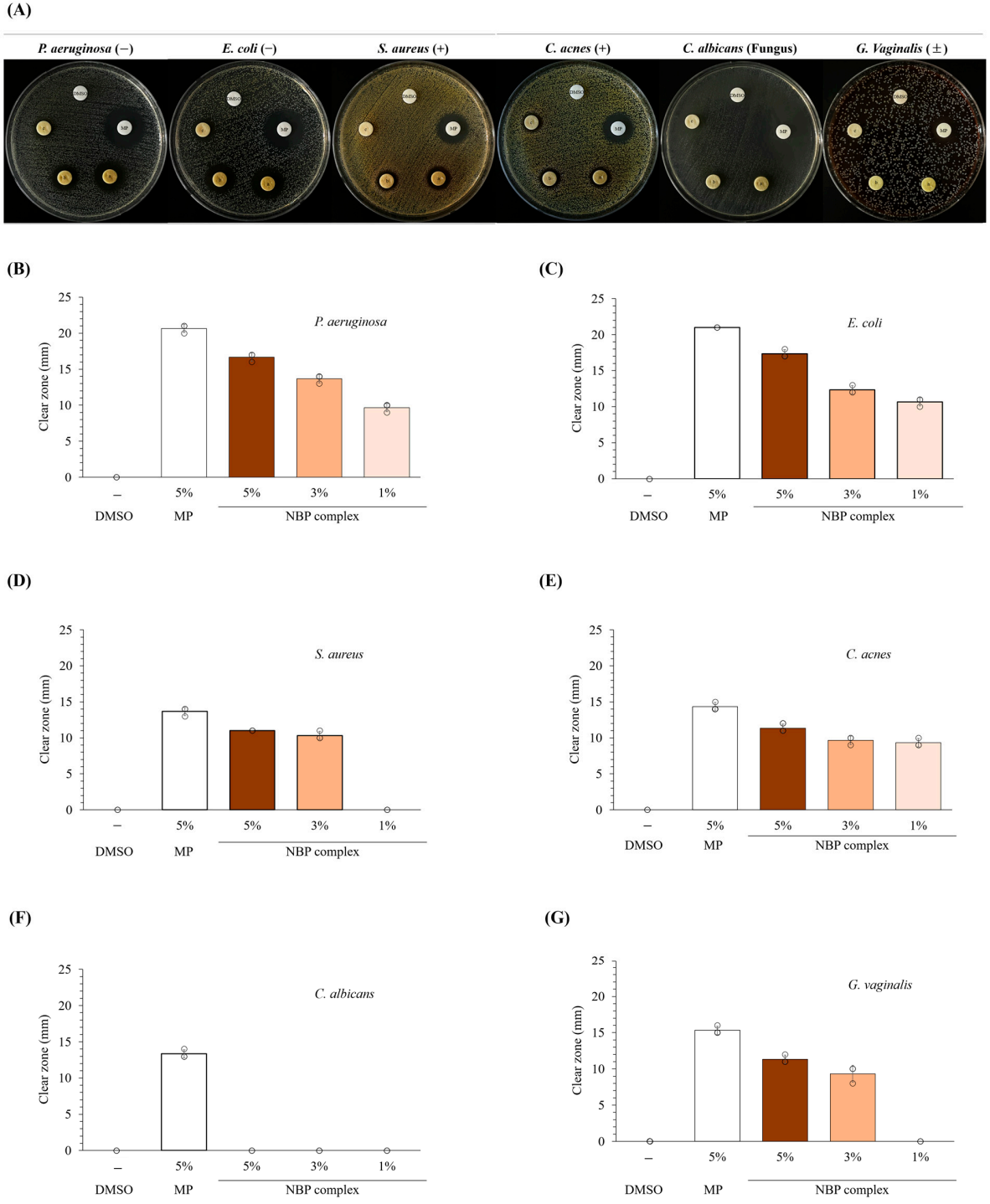


Figure 9. Antimicrobial Activity of NBP Complex. (**A**) Representative images of inhibition zones on agar plates. Positive control: methyl paraben (MP), negative control: dimethyl sulfoxide (DMSO). Paper disk size: 8 mm. a: 5% of NBP complex, b: 3% of NBP complex, c: 1% of NBP complex. (**B**) *P. aeruginosa*;

(**C**) *E. coli*; (**D**) *S. aureus*; (**E**) *C. acnes*; (**F**) *C. albicans*; (**G**) *G. vaginalis*. All statistical analyses were conducted with Microsoft Excel software. Data represents the mean ± SD. Each circle represents an individual data point from independent samples.

4. Discussion

During the extraction of NBPs, it was observed that *M. pumila* (pomace), *P. pyrifolia* (pomace), and *S. japonica* (discarded thallus) exhibited noticeably higher yields compared to other extracts. This unusual observation during the experiments prompted a focus on the notably high extraction yields of these samples to explore the factors underlying their enhanced extraction efficiency. Investigation of their common characteristics revealed a high content of water-soluble polysaccharides. Water-soluble polysaccharides contain abundant hydroxyl groups (-OH) within their molecular structures, which confer high hydrophilicity. This structural feature promotes interactions with solvents, enhancing solubility, and consequently facilitating the extraction of water-soluble components from polysaccharide-rich samples [30,31].

In the case of fruit by-products (*M. pumila* (pomace), *P. pyrifolia* (pomace)), it was observed that they formed viscous solids upon freeze-drying. This property is attributed to their high content of sugars and pectins, which increases the proportion of extractable components during solvent extraction, resulting in higher yields [32,33]. Although not a fruit by-product, *S. japonica* (discarded thallus), which also exhibited high extraction yields, was further analyzed. Similar to fruit pomace, brown algae like *S. japonica* are known to be rich in water-soluble polysaccharides such as alginate, fucoidan, and laminaran [34,35].

However, unlike fruit pomace, *S. japonica* formed a powder upon drying. This difference is due to variations in the types of sugars and structural characteristics of polysaccharides between the two categories. Sugars in fruit pomace primarily consist of monosaccharides like fructose and glucose or disaccharides. Previous studies reported that the total sugar content of *M. pumila* (pomace) ranged from 46% to 69% [36], with approximately 49.86 g/100 g of fructose in dried *M. pumila* (pomace) [37]. In *P. pyrifolia* (pomace), fructose predominates among the sugars, followed by glucose and sucrose [38]. These low-molecular-weight sugars exhibit high hygroscopicity and stickiness, contributing to the clumping of extracts [39].

In contrast, *S. japonica* contains low amounts of these low-molecular-weight sugars, and its water-soluble polysaccharides are of high molecular weight with low hydrophilicity. Notably, the major component, alginate, forms gels upon contact with water and binds with minerals such as calcium and sodium to form a stable three-dimensional gel matrix, limiting water absorption [40–42]. Conversely, pectin in fruit pomace contains numerous hydrophilic functional groups such as hydroxyl (-OH) and carboxyl (-COOH) groups, which can form hydrogen bonds with water molecules, facilitating water adsorption and, in combination with sugars, contributing to clumping and stickiness [43].

Despite the high extraction yields and favorable physicochemical properties of these extracts, their biological activities were found to be relatively low. In contrast, the four extracts that demonstrated notable bioactivity—*A. hypogaea* (shell), *S. angulatus* (whole plant), *A. cepa* (peel), and *C. obtusa* (root)—exhibited low to moderate extraction yields of 2.11%, 6.04%, 8.83%, and 6.40%, respectively. These findings further suggest that extraction yield does not necessarily correlate with biological activity. Consequently, while extraction efficiency provides useful information for material recovery, comprehensive evaluation of bioactive properties remains essential for identifying extracts suitable for composite formulations with enhanced functional effects. Therefore, future studies should integrate both yield and bioactivity data to guide the rational design of multi-component extracts.

In the present study, antimicrobial activity was evaluated not from a clinical therapeutic perspective, but as an initial screening to assess the functional properties and potential industrial applications of natural product derived materials. Given this objective, the use of conventional antibiotics as positive controls may not provide an appropriate benchmark, as their highly specific mechanisms of action limit direct comparison with the broad-spectrum and non-specific antimicrobial effects observed in preliminary evaluations of plant extracts. In contrast, MP exhibits antimicrobial activity against a wide range of microorganisms, including both Gram-positive and Gram-negative bacteria, and has been widely used as a non-antibiotic preservative across the cosmetics, food, and pharmaceutical industries [44,45]. Therefore, in the present study, MP was employed as a positive control to enhance the practical relevance of the experimental results and the validity of their interpretation.

In the field of natural product research, initial cytotoxicity evaluations have been reported to serve as a basis for subsequent investigations exploring a range of bioactivities, including studies employing cancer cell models. Compounds that reduce cell viability are particularly likely to possess biological activities related to cell proliferation regulation and apoptosis induction [46,47]. In this context, the extracts of *A. cepa* (peel) and *C. obtusa* (root), which exhibited relatively high cytotoxicity in the present study, may be considered promising candidates for further mechanistic studies, including those involving tumor cell-based models, to expand the evaluation of their bioactive potential.

The concentrations used were selected based on (i) commonly applied screening levels in natural-product research and (ii) preliminary cell-viability results to ensure non-cytotoxic ranges. Individual extracts were mainly evaluated at defined screening concentrations, whereas the complex was examined within non-cytotoxic ranges. Full dose–response curves for all single extracts were beyond the scope of this work and will be addressed in future studies. The scoring system described in Section 2.13 was calculated using results obtained at the predefined screening concentrations in each assay, and it did not combine data generated at different concentration levels.

This study has certain limitations, as it was conducted under restricted in vitro conditions and specific concentration ranges. The results should be interpreted as exploratory indicators, providing a relative comparison of trends rather than an absolute quantitative assessment of potency. The scoring system, while useful for preliminary screening, may not fully capture the distinct biological relevance of heterogeneous assays like antioxidant and antimicrobial activities. Therefore, further standardized quantitative analyses and mechanistic evaluations are warranted to elucidate the molecular pathways of the identified candidates. For the NBP complex, future investigations should focus on assessing synergistic interactions and identifying key active components.

Despite these limitations, this study is significant for re-evaluating industrial by-products as high-value functional materials. By scientifically verifying the multifunctional potential of 12 natural by-products, we provide a foundation for transitioning these underutilized resources into advanced composite formulations. This initial screening serves as a critical stepping stone for future applied research in functional material development.

5. Conclusions

This study demonstrates the potential of plant by-products, which are often discarded through incineration or landfilling, to serve as multifunctional bioactive materials. Among residues collected from various regions in Republic of Korea, *A. hypogaea* (shell), *C. obtusa* (root), *A. cepa* (peel), and *S. angulatus* (whole plant) were selected based on their superior performance in overall bioactivity assessment, antibacterial activity, and anti-inflammatory effects. The composite extract, prepared based on RAW 264.7 cell viability results, exhibited

significant antibacterial activity, particularly against *E. coli* and *P. aeruginosa*, and effectively inhibited NO production as well as the inflammatory mediators iNOS and COX-2 at 50 and 100 μg/mL. These results underscore both the functional and environmental benefits of repurposing plant residues. Considering the ecological impact of conventional disposal methods, this study highlights the importance of sustainable utilization of by-products and provides a foundation for future research on their development as multifunctional bioactive materials.

Supplementary Materials: The following supporting information can be downloaded at: https://www.mdpi.com/article/10.3390/nutraceuticals6020021/s1, Figure S1: Western blot whole band in Figure 8; Figure S2: HPLC fingerprint profiles of selected plant extracts with bioactive potential; Table S1: Detailed HPLC condition.

Author Contributions: Conceptualization, Y.-J.K.; methodology, N.-H.P. and J.-A.B.; investigation, N.-H.P., J.-A.B., M.-P.J., S.Y. and J.-Y.K.; resources, G.H.K.; writing—original draft preparation, N.-H.P. and Y.-J.K.; writing—review and editing, N.-H.P., J.-A.B., B.-A.K. and Y.-J.K.; supervision, Y.-J.K.; project administration, N.-H.P., J.-A.B. and Y.-J.K. All authors have read and agreed to the published version of the manuscript.

Funding: This research was supported by the Regional Innovation System & Education (RISE) program through the Institute for Regional Innovation System & Education in Busan Metropolitan City, funded by the Ministry of Education (MOE) and the Busan Metropolitan City, Republic of Korea (2026-RISE-02-005-001).

Informed Consent Statement: Not applicable.

Data Availability Statement: The data presented in this study are available from the corresponding author upon reasonable request.

Conflicts of Interest: Author Seulki Yoon was employed by the company OATC Skin Clinical Trial Center, Seoul, Republic of Korea, and author Gyu Hoon Kim was employed by the company Skinhealth Cosmetic Co., Ltd., Busan, Republic of Korea. The remaining authors declare that the research was conducted in the absence of any commercial or financial relationships that could be construed as a potential conflict of interest.

Abbreviations

The following abbreviations are used in this manuscript:

A. cepa	*Allium cepa* L.
A. hypogaea	*Arachis hypogaea* L.
AA	Ascorbic acid
ABTS	2,2′-azino-bis(3-ethylbenzothiazoline-6-sulfonic acid)
BHA	Butylated hydroxyanisole
C. acnes	*Cutibacterium acnes*
C. albicans	*Candida albicans*
C. obtusa	*Chamaecyparis obtusa* (Siebold & Zucc.) Endl.
COOH	Carboxyl group
COX-2	Cyclooxygenase-2
DMEM	Dulbecco's Modified Eagle Medium
DMSO	Dimethyl sulfoxide
DPPH	2,2-diphenyl-1-picrylhydrazyl
E. coli	*Escherichia coli*
FBS	Fetal bovine serum
G. vaginalis	*Gardnerella vaginalis*
HRP	Horseradish peroxidase
iNOS	Inducible nitric oxide synthase

L-DOPA	L-3,4-dihydroxyphenylalanine
LPS	Lipopolysaccharide
M. pumila	*Malus pumila* Mill.
MP	Methyl paraben
MTT	3-(4,5-dimethylthiazol-2-yl)-2,5-diphenyltetrazolium bromide
NBPs	Natural by-products
NO	Nitric oxide
OH	Hydroxyl group
$ONOO^-$	Peroxynitrite
P. aeruginosa	*Pseudomonas aeruginosa*
P. pyrifolia	*Pyrus pyrifolia* var. *cultiva* (Makino) Nakai
PBS	Phosphate-buffered saline
ROS	Reactive oxygen species
S. angulatus	*Sicyos angulatus* L.
S. aureus	*Staphylococcus aureus*
S. japonica	*Saccharina japonica* (Areschoug) C.E. Lane, C. Mayes, Druehl & G.W. Saunders
SDS-PAGE	Sodium dodecyl sulfate–polyacrylamide gel electrophoresis
UA	Ursolic acid
Z. mays	*Zea mays* L.

References

1. Błaszczyk, A.; Sady, S.; Pachołek, B.; Jakubowska, D.; Grzybowska-Brzezińska, M.; Krzywonos, M.; Popek, S. Sustainable Management Strategies for Fruit Processing Byproducts for Biorefineries: A Review. *Sustainability* **2024**, *16*, 1717. [CrossRef]
2. Santos, L.F.D.; Lopes, S.T.; Nazari, M.T.; Biduski, B.; Pinto, V.Z.; Santos, J.S.D.; Bertolin, T.E.; Santos, L.R.D. Fruit Pomace as a Promising Source to Obtain Biocompounds with Antibacterial Activity. *Crit. Rev. Food Sci. Nutr.* **2023**, *63*, 12597–12609. [CrossRef]
3. Zeng, Y.; Zhou, W.; Yu, J.; Zhao, L.; Wang, K.; Hu, Z.; Liu, X. By-Products of Fruit and Vegetables: Antioxidant Properties of Extractable and Non-Extractable Phenolic Compounds. *Antioxidants* **2023**, *12*, 418. [CrossRef]
4. Roy, P.; Mohanty, A.K.; Dick, P.; Misra, M. A Review on the Challenges and Choices for Food Waste Valorization: Environmental and Economic Impacts. *ACS Environ. Au* **2023**, *3*, 58–75. [CrossRef] [PubMed]
5. Bak, M.-J.; Hong, S.-G.; Lee, J.-W.; Jeong, W.-S. Red Ginseng Marc Oil Inhibits iNOS and COX-2 via NFκB and P38 Pathways in LPS-Stimulated RAW 264.7 Macrophages. *Molecules* **2012**, *17*, 13769–13786. [CrossRef] [PubMed]
6. Li, Y.-N.; Wu, Y.-L.; Jia, Z.-H.; Qi, J.-S. Interaction between COX-2 and iNOS Aggravates Vascular Lesion and Antagonistic Effect of Ginsenoside. *J. Ethnopharmacol.* **2008**, *119*, 305–311. [CrossRef] [PubMed]
7. Korbecki, J.; Baranowska-Bosiacka, I.; Gutowska, I.; Chlubek, D. The Effect of Reactive Oxygen Species on the Synthesis of Prostanoids from Arachidonic Acid. *J. Physiol. Pharmacol. Off. J. Pol. Physiol. Soc.* **2013**, *64*, 409–421.
8. Huang, C.; Zhuo, F.; Han, B.; Li, W.; Jiang, B.; Zhang, K.; Jian, X.; Chen, Z.; Li, H.; Huang, H.; et al. The Updates and Implications of Cutaneous Microbiota in Acne. *Cell Biosci.* **2023**, *13*, 113. [CrossRef]
9. Kim, J.; Ochoa, M.-T.; Krutzik, S.R.; Takeuchi, O.; Uematsu, S.; Legaspi, A.J.; Brightbill, H.D.; Holland, D.; Cunliffe, W.J.; Akira, S.; et al. Activation of Toll-Like Receptor 2 in Acne Triggers Inflammatory Cytokine Responses1. *J. Immunol.* **2002**, *169*, 1535–1541. [CrossRef]
10. Liu, Q.; Mazhar, M.; Miller, L.S. Immune and Inflammatory Reponses to Staphylococcus Aureus Skin Infections. *Curr. Dermatol. Rep.* **2018**, *7*, 338–349. [CrossRef]
11. Rasquel-Oliveira, F.S.; Ribeiro, J.M.; Martelossi-Cebinelli, G.; Costa, F.B.; Nakazato, G.; Casagrande, R.; Verri, W.A. *Staphylococcus aureus* in Inflammation and Pain: Update on Pathologic Mechanisms. *Pathogens* **2025**, *14*, 185. [CrossRef]
12. Sahu, A.; Ruhal, R. Immune System Dynamics in Response to *Pseudomonas aeruginosa* Biofilms. *NPJ Biofilms Microbiomes* **2025**, *11*, 104. [CrossRef]
13. Trøstrup, H.; Thomsen, K.; Christophersen, L.J.; Hougen, H.P.; Bjarnsholt, T.; Jensen, P.Ø.; Kirkby, N.; Calum, H.; Høiby, N.; Moser, C. *Pseudomonas aeruginosa* Biofilm Aggravates Skin Inflammatory Response in BALB/c Mice in a Novel Chronic Wound Model. *Wound Repair Regen.* **2013**, *21*, 292–299. [CrossRef]
14. Petkovšek, Ž.; Eleršič, K.; Gubina, M.; Žgur-Bertok, D.; Starčič Erjavec, M. Virulence Potential of *Escherichia coli* Isolates from Skin and Soft Tissue Infections. *J. Clin. Microbiol.* **2009**, *47*, 1811–1817. [CrossRef]
15. Machado, A.; Cerca, N. Influence of Biofilm Formation by *Gardnerella vaginalis* and Other Anaerobes on Bacterial Vaginosis. *J. Infect. Dis.* **2015**, *212*, 1856–1861. [CrossRef] [PubMed]

16. Palese, E.; Nudo, M.; Zino, G.; Devirgiliis, V.; Carbotti, M.; Cinelli, E.; Rodio, D.M.; Bressan, A.; Prezioso, C.; Ambrosi, C.; et al. Cutaneous Candidiasis Caused by *Candida albicans* in a Young Non-Immunosuppressed Patient: An Unusual Presentation. *Int. J. Immunopathol. Pharmacol.* **2018**, *32*, 2058738418781368. [CrossRef] [PubMed]
17. Kedare, S.B.; Singh, R.P. Genesis and Development of DPPH Method of Antioxidant Assay. *J. Food Sci. Technol.* **2011**, *48*, 412–422. [CrossRef] [PubMed]
18. Re, R.; Pellegrini, N.; Proteggente, A.; Pannala, A.; Yang, M.; Rice-Evans, C. Antioxidant Activity Applying an Improved ABTS Radical Cation Decolorization Assay. *Free Radic. Biol. Med.* **1999**, *26*, 1231–1237. [CrossRef] [PubMed]
19. Azmi, N.; Hashim, P.; Hashim, D.M.; Halimoon, N.; Majid, N.M.N. Anti-Elastase, Anti-Tyrosinase and Matrix Metalloproteinase-1 Inhibitory Activity of Earthworm Extracts as Potential New Anti-Aging Agent. *Asian Pac. J. Trop. Biomed.* **2014**, *4*, S348–S352. [CrossRef]
20. Park, J.H.; Shin, J.Y.; Heo, J.H.; Kim, S.J.; Kim, S.J.; Jeong, S.Y.; Kim, A.J.; Jang, S.I.; Cho, B.O. Antioxidant, anti-inflammatory, anti-collagenase, and anti-elastase effects of fermented *Astragalus membranaceus* extracts. *Korean J. Food Sci. Technol.* **2024**, *56*, 320–327. [CrossRef]
21. Kumar, P.; Nagarajan, A.; Uchil, P.D. Analysis of Cell Viability by the MTT Assay. *Cold Spring Harb. Protoc.* **2018**, *2018*, pdb-prot095505. [CrossRef]
22. Kim, C.-H.; Kwon, Y.-J.; Jang, Y.-A. Anti-Inflammatory Effects of *Chamaecyparis obtusa* (Siebold & Zucc.) Endl. Leaf Extract Fermented by Ganoderma Applanatum Mycelia. *Pharmaceutics* **2024**, *16*, 365. [CrossRef]
23. Kim, B.-A.; Byeon, J.-A.; Jang, Y.-A.; Kwon, Y.-J.; Kim, B.-A.; Byeon, J.-A.; Jang, Y.-A.; Kwon, Y.-J. Bark Extracts of *Chamaecyparis obtusa* (Siebold & Zucc.) Endl. Attenuate LPS-Induced Inflammatory Responses in RAW264.7 Macrophages. *Plants* **2025**, *14*, 2346. [CrossRef]
24. Kim, S.-H.; Jang, Y.-A.; Kwon, Y.-J. Anti-Inflammatory Effect of *Chamaecyparis obtusa* (Siebold & Zucc.) Endl. Leaf Essential Oil. *Molecules* **2024**, *29*, 1117. [CrossRef]
25. Sule, R.; Rivera, G.; Gomes, A.V. Western Blotting (Immunoblotting): History, Theory, Uses, Protocol, and Problems. *BioTechniques* **2023**, *75*, 99–114. [CrossRef] [PubMed]
26. Ngamsurach, P.; Praipipat, P. Antibacterial Activities against *Staphylococcus aureus* and *Escherichia coli* of Extracted *Piper betle* Leaf Materials by Disc Diffusion Assay and Batch Experiments. *RSC Adv.* **2022**, *12*, 26435–26454. [CrossRef] [PubMed]
27. Sain, A.A.; Amanah, A.; Noor, M.H.M.; Lau, W.K.; Abayomi, O.O.; Zainuddin, Z. Establishment of High-Throughput Screening Assay Using 384-Well Plate for Identification of Potent Antioxidants from Malaysian Local Plants Repository and Phytochemical Profile of Tetracera Scandens. *Trop. Life Sci. Res.* **2025**, *36*, 23–57. [CrossRef]
28. Chiocchio, I.; Mandrone, M.; Sanna, C.; Maxia, A.; Tacchini, M.; Poli, F. Screening of a Hundred Plant Extracts as Tyrosinase and Elastase Inhibitors, Two Enzymatic Targets of Cosmetic Interest. *Ind. Crops Prod.* **2018**, *122*, 498–505. [CrossRef]
29. Zhang, X.-J.; Diao, M.-N.; Zhang, Y.-F. A Review of the Occurrence, Metabolites and Health Risks of Butylated Hydroxyanisole (BHA). *J. Sci. Food Agric.* **2023**, *103*, 6150–6166. [CrossRef]
30. Zhao, B.; Liu, J.; Chen, X.; Zhang, J.; Wang, J. Purification, Structure and Anti-Oxidation of Polysaccharides from the Fruit of Nitraria Tangutorum Bobr. *RSC Adv.* **2018**, *8*, 11731–11743. [CrossRef]
31. Jeffree, C.E. Immobilization of Pectin, Xyloglucan and Other Soluble Plant Polysaccharides on Blotting Membranes. *New Phytol.* **1993**, *125*, 695–706. [CrossRef] [PubMed]
32. Putra, N.R.; Rizkiyah, D.N.; Abdul Aziz, A.H.; Che Yunus, M.A.; Veza, I.; Harny, I.; Tirta, A. Waste to Wealth of Apple Pomace Valorization by Past and Current Extraction Processes: A Review. *Sustainability* **2023**, *15*, 830. [CrossRef]
33. Yikilkan, Y.; Redha, A.A.; Kaba, B.; Pasazadeh, H.; Koca, I. Production of Chokeberry Pulp Powder by Convective and Freeze-Drying Foam-Mat Techniques: Effects on Physicochemical Properties, Bioactive Content, and Antioxidant Activity. *Sustain. Food Technol.* **2025**, *3*, 1329–1340. [CrossRef]
34. Dobrinčić, A.; Balbino, S.; Zorić, Z.; Pedisić, S.; Kovačević, D.B.; Garofulić, I.E.; Dragović-Uzelac, V. Advanced Technologies for the Extraction of Marine Brown Algal Polysaccharides. *Mar. Drugs* **2020**, *18*, 168. [CrossRef]
35. Mohd Fauziee, N.A.; Chang, L.S.; Wan Mustapha, W.A.; Md Nor, A.R.; Lim, S.J. Functional Polysaccharides of Fucoidan, Laminaran and Alginate from Malaysian Brown Seaweeds (Sargassum Polycystum, Turbinaria Ornata and Padina Boryana). *Int. J. Biol. Macromol.* **2021**, *167*, 1135–1145. [CrossRef]
36. Bindon, K.; Qi, S.; Kassara, S.; Nicolotti, L.; Jouin, A.; Beer, M. Apple Pomace Compositional Data Highlighting the Proportional Contribution of Polymeric Procyanidins. *Molecules* **2023**, *28*, 5494. [CrossRef]
37. Sudha, M.L.; Dharmesh, S.M.; Pynam, H.; Bhimangouder, S.V.; Eipson, S.W.; Somasundaram, R.; Nanjarajurs, S.M. Antioxidant and Cyto/DNA Protective Properties of Apple Pomace Enriched Bakery Products. *J. Food Sci. Technol.* **2016**, *53*, 1909–1918. [CrossRef] [PubMed]
38. Chen, J.; Wang, Z.; Wu, J.; Wang, Q.; Hu, X. Chemical Compositional Characterization of Eight Pear Cultivars Grown in China. *Food Chem.* **2007**, *104*, 268–275. [CrossRef]
39. Baroyi, S.A.H.M.; Rosland Abel, S.E.; Al-Awaadh, A.M.; Fikry, M.; Shah, N.N.A.K.; Mohd Salleh, F.S.; Garg, V.; Deng, T.; Yusof, Y.A. Sweet Flow: Exploring the Flowability, Caking, Morphology, and Solubility of Date Sugars as Promising Sugar Substitutes. *Powder Technol.* **2024**, *443*, 119925. [CrossRef]

40. Wang, Q.-Q.; Liu, Y.; Zhang, C.-J.; Zhang, C.; Zhu, P. Alginate/Gelatin Blended Hydrogel Fibers Cross-Linked by Ca^{2+} and Oxidized Starch: Preparation and Properties. *Mater. Sci. Eng. C* **2019**, *99*, 1469–1476. [CrossRef] [PubMed]
41. Sıçramaz, H.; Dönmez, A.B.; Güven, B.; Ünal, D.; Aşbay, E. Microstructure and Release Behavior of Alginate–Natural Hydrocolloid Composites: A Comparative Study. *Polymers* **2025**, *17*, 531. [CrossRef]
42. Jeong, C.; Jo, E.-H.; Kim, S.-B.; Cho, S. Effects of Xanthan Gum Treatment on the Quality and Stability of Imitation Fish Roe Based on Calcium Alginate Hydrogels. *Korean J. Fish. Aquat. Sci.* **2020**, *53*, 583–587. [CrossRef]
43. Nguyen, H.H.D.; Nguyen, H.V.H.; Savage, G.P. Properties of Pectin Extracted from Vietnamese Mango Peels. *Foods* **2019**, *8*, 629. [CrossRef] [PubMed]
44. Głaz, P.; Rosińska, A.; Woźniak, S.; Boguszewska-Czubara, A.; Biernasiuk, A.; Matosiuk, D. Effect of Commonly Used Cosmetic Preservatives on Healthy Human Skin Cells. *Cells* **2023**, *12*, 1076. [CrossRef] [PubMed]
45. Soni, M.G.; Taylor, S.L.; Greenberg, N.A.; Burdock, G.A. Evaluation of the Health Aspects of Methyl Paraben: A Review of the Published Literature. *Food Chem. Toxicol.* **2002**, *40*, 1335–1373. [CrossRef] [PubMed]
46. Chunarkar-Patil, P.; Kaleem, M.; Mishra, R.; Ray, S.; Ahmad, A.; Verma, D.; Bhayye, S.; Dubey, R.; Singh, H.N.; Kumar, S. Anticancer Drug Discovery Based on Natural Products: From Computational Approaches to Clinical Studies. *Biomedicines* **2024**, *12*, 201. [CrossRef]
47. Setiawati, A.; Candrasari, D.S.; Setyajati, F.D.E.; Prasetyo, V.K.; Setyaningsih, D.; Hartini, Y.S. Anticancer Drug Screening of Natural Products: In Vitro: Cytotoxicity Assays, Techniques, and Challenges. *Asian Pac. J. Trop. Biomed.* **2022**, *12*, 279. [CrossRef]

Disclaimer/Publisher's Note: The statements, opinions and data contained in all publications are solely those of the individual author(s) and contributor(s) and not of MDPI and/or the editor(s). MDPI and/or the editor(s) disclaim responsibility for any injury to people or property resulting from any ideas, methods, instructions or products referred to in the content.